American Mineralogist, Volume 64, pages 424–431, 1979

Layer deformation and crystal energy of micas and related minerals. II. Deformation of the coordination units

C. ANTON J. APPELO

Instituut voor Aardwetenschappen, Vrije Universiteit
De Boelelaan 1085, Amsterdam

Abstract

Electrostatic energy calculations are made to investigate distortions in the mica structure. The use of the electrostatic model is valid to explain 99 percent of the variation of K–O bondlengths in structure refinements. The interlayer cation has little influence on tetrahedral rotation, because its site has a more favorable potential as the tetrahedral rotation decreases and the tetrahedra are elongated. It is suggested that the tetrahedral elongation is larger when the positive tetrahedral charge is lower. This is confirmed by phlogopite refinements. It is suggested that a larger octahedral cation diminishes the counter-rotation of upper and lower oxygen triads in the dioctahedral layer. This "octahedral rotation" deforms the tetrahedral layer, and determines the relative stability of the 1M and $2M_1$ polytypes. The 1M polytype would be more stable by less than 0.2 kcal if the octahedral rotation remains less than 4°. The larger octahedral cations in glauconite and celadonite explain the exclusive occurrence of these minerals as 1M polytypes.

Introduction

Electrostatic energy calculations have been applied quite successfully to the alkali halogenides (Born and Huang, 1954; Tosi, 1964), and to other simple ionic structures (Waddington, 1959; Busing, 1970). The application of these calculations to silicates has been relatively rare, perhaps because it takes too much time to do the more complex structures by hand. The high-speed computer permits the more powerful molecular orbital calculations, even if this approach would require excessive amounts of computing time when compared with electrostatic calculations.

Apart from this, published results of electrostatic calculations show them to be useful in explaining the crystal chemistry of silicates. Outstanding examples are found in the literature on the electrostatic control of structural distortions in garnets (Born and Zemann, 1964) and zircon (Sahl and Zemann, 1965), and in the work by Hartman (1972) and co-workers (Felius, 1976; 't Hart, 1978) in explaining crystal morphology. Ohashi and Burnham (1972) applied the method to investigate cation-site distribution in pyroxene, and Giese (1971) has successfully located proton positions in muscovite. Of related interest is the work on exfoliation of the mica structure (Giese, 1974, 1975; Appelo, 1977), and a potential map of the interlayer region of vermiculite (Hougardy *et al.*, 1976).

There are various methods of approach for the more complex structures: one may proceed from individual site-energies, where differences indicate ordering (Ohashi and Burnham, 1972); one may correct for a partial covalent character of certain bonds, as is customary for the Si–O bond (Sahl and Zemann, 1965); and it is possible to use models for the calculation of the repulsive energy which include empirical and adjustable variables (Tosi, 1964; Busing, 1970). This ambiguous character of the electrostatic model may be resolved to some extent when sufficient thermochemical data become available, but at present only a comparative method can be used.

It nevertheless offers one way of investigating the complex compositional variations of rock-forming silicates from a structural point of view, if only relative energy effects of distortions are considered. In the present study the method is applied to the structural models of micas given earlier (Appelo, 1978). To be discussed are the effects of (1) flattening of the octahedral layer (accompanied by a larger b, or decreasing octahedral rotation), (2) lengthening of the tetrahedra (compensated for by decreasing the tetrahedral rotation), and (3) coordination around the interlayer cation in 1M and $2M_1$ polytypes. Elec-

0003–004X/79/0304–0424$02.00

trostatic calculations will be given also for micas with refined structures.

Calculation of the crystal energy

The direct summation of the Coulomb energy of a crystal lattice,

$$E = \tfrac{1}{2} \sum_n \sum_m Q_n Q_m / r_{n-m}$$

is proceeding only slowly, and several mathematical manipulations have been devised to accelerate the convergency rate (*cf.* Tosi, 1964).

The methods of Ewald (1921) and Bertaut (1952) are generally applicable for the more complicated structures. The Ewald method converges somewhat more rapidly if an accuracy higher than 1 part per thousand is required (Born and Zemann, 1964). Kittel (1956, p. 571–574) gives a particularly lucid derivation of the Ewald method, which is used here. The essential line of thought is that if Gaussian charge distributions of reversed sign of charge are superimposed on the point charges, this easily adds up as a complementary error-function to the lattice site, the potential of which is to be calculated. The Gaussian charge distributions are neutralized again by summing up an identical Gaussian distribution, which is now of the same sign of charge as the point charges, and can be written as a Fourier series in the reciprocal lattice. By summing up a Gaussian charge distribution of reduced peak height, the convergency is appreciably more rapid than for a Fourier series of the point charges. The use of different half-widths of the Gaussian distribution should not affect the results, which enables testing the computer programming and calculation. An accuracy higher than 10^{-4} e/A is obtained for the 1M (resp. $2M_1$) structure, with a half-width of 0.84 (0.92)A, an error-function calculated for anion–anion and cation–anion contacts <2.6 (2.9)A, and with a Fourier series up to 1.42 (1.3)/A^2. The electrostatic energy or Madelung sum of the structure, based here on 12 anions, is obtained by multiplication of the potentials with the charge of the ion at the specific site.

The repulsive energy is estimated with a model given by Pauling (1960, p. 523):

$$W_{rep.} = \tfrac{1}{2} \sum_n \sum_m \beta_{nm} B (r_n + r_m)^8 / r_{n-m}^9$$

where: $\beta_{nm} = 1 + Q_n/P_n + Q_m/P_m$, $Q_{n,m}$ being the formal charge, $P_{n,m}$ being the number of outer electrons of n,m. B = repulsive coefficient, given the value 0.03 e^2. r_{n-m} = interionic distance between n and m. The standard-radii $r_{n,m}$ of alkali and halogenide ions calculated by this formula show a good agreement with Pauling's set of crystal radii derived from quantum-chemical arguments (Pauling, 1960, p. 514, 526). The use of these crystal radii thus makes it a model which is easily applicable for those ions and compounds for which more precise data (especially thermochemical data) are lacking. The crystal radii are multiplied by $Q^{0.25}$, as suggested by Pauling (p. 526). Van der Waals energy and terms of still higher order are neglected, as in Pauling's approach, although they will be incorporated in part in the repulsive terms.

The Born-Haber value of the enthalpy of formation of the phlogopite described by McCauley *et al.* (1973), with all elements fully ionized and this repulsive energy, was found to be fairly close to the thermochemical value (Appelo, 1977). This may indicate a far more highly ionic Si–O bond than is found when using Pauling's (1960, p. 98) model, or molecular orbital calculations (Tossell, 1977). Although a similarly highly ionic Si–O bond has been suggested before (Verhoogen, 1958; Gait and Ferguson, 1970), the presently-known molecular orbital results possibly have a greater significance. Therefore the calculations have been made with different charges imposed on silicon and the coordinating oxygens. The effective charge of the tetrahedral cation then becomes $Q_M(4) = Q'_{Si} + f_{Al}(3 - Q'_{Si})$, with Al holding its formal charge, and Q'_{Si} being the chosen charge on Si. The charge of the basal oxygens changes accordingly to $Q_{Ob} = -2 + (1 - f_{Al})(4 - Q'_{Si})/2$, and of the apical oxygens to $Q_{Oa} = -2 + (1 - f_{Al})(4 - Q'_{Si})/4$.

Deformation energies

In order to be able to separate deformation energies over the coordination units, it is assumed that the geometry of the individual tetrahedron will not be affected when the octahedral coordination is distorted, and *vice versa*. The structural deformations always are interdependent (in line with the proposed geometrical models), which solely permits a discussion of the combined effects on the crystal energy. Consistent results were obtained nevertheless, when the geometry of the independent coordination unit was varied. The explanation is seen in the dominant influence of the directly coordinating ions on the crystal energy. The interlayer region forms an exception to the fixed geometrical units, in the sense that the K–O bondlengths vary with tetrahedral rotation according to a fixed relation (Appelo, 1978).

Octahedral layer

Two commonly occurring deformations of the oc-

tahedral layer in micas have been formalized geometrically, *viz.* flattening of the octahedra into trigonal antiprisms, and a counter-rotation of upper and lower oxygen triads in the dioctahedral layer called octahedral rotation. These deformations affect both the tetrahedral layer and the interlayer region. Flattening of the octahedral layer increases the lateral dimensions of the 1M model unit cell, if octahedral cation–oxygen bondlengths remain the same. Both flattening and octahedral rotation may occur in the $2M_1$ model without affecting the lateral dimensions, but changing the amount of tetrahedral tilting.

The results of electrostatic calculations for the 1M model are difficult to apply. The crystal energy of a trioctahedral mica decreases with decreasing b (9.25–9.10A) and increasing expansion of the octahedral layer, when corrected for the changing octahedral O–O and interlayer K–O repulsion energies. If the hydroxyl group is replaced by fluorine, the opposite result is obtained. Although electrostatic calculations cannot explain a fixed b associated with different octahedral cations (except in terms of a certain OH/F ratio), the calculations suggest that phlogopite will have smaller lateral dimensions than fluor-phlogopite of otherwise equal composition; this is not, or at least not clearly, observed (Noda and Yamanishi, 1964).

The exchange of hydroxyl for fluorine is associated with a marked decrease in c' (Yoder and Eugster, 1954; Noda and Yamanishi, 1964; Munoz and Ludington, 1974), which is rather peculiar, since structure refinements do not indicate particularly shorter K–O distances for fluor-phlogopite (Table 1, Appelo, 1978), and since the other bondlengths which affect unit-cell dimensions are likely to remain equal as well. Hydrogenation of oxy-biotite increases c' by only 0.09A (Takeda and Ross, 1975), and part of this increase is due to the increase of $r^{(6)}_{M-O}$ when Fe^{3+} is reduced, and b remains the same. This evidence also suggests that the significant decrease of c' which results from the hydroxyl/fluorine exchange is caused by an increase of the lateral dimensions.

For the dioctahedral $2M_1$ micas it was found that the Madelung sum increased with increasing octahedral rotation for constant b and $r^{(6)}_{M-O}$ (Fig. 1). The repulsive energy however shows a well-defined minimum, which tends to dominate the crystal energy. The results are shown in Figure 1 for $r^{(6)}_{Al-O} = 1.92$A. They indicate that it is electrostatically favorable, when the lateral dimensions of the unit cell increase simultaneously with the octahedral rotation. A fixed $b = 9.00$A for muscovite is therefore not explained, although the energy differences tend to become small, and indeed even lower than the effects of octahedral

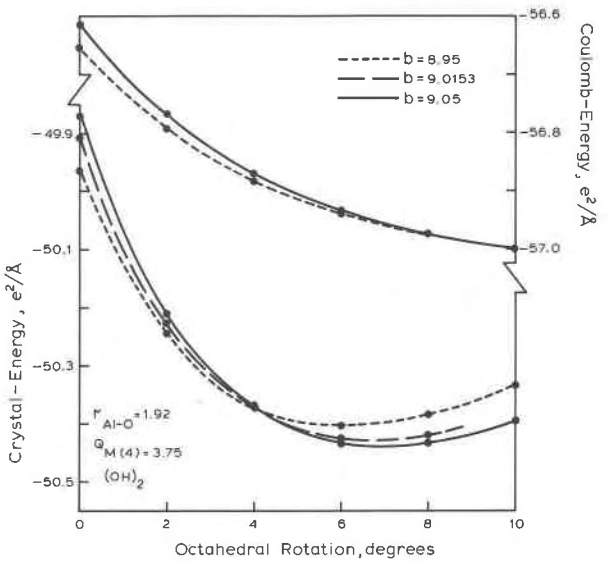

Fig. 1. Coulomb energy and repulsion-corrected crystal energy of muscovite as a function of the rotation of octahedral oxygen triads. The crystal energy is not corrected for Al–O and O–H repulsive energies, which remain constant with constant bondlengths.

rotation. Since the calculated optimum rotation does fit the structure refinements quite well, it is attractive to explain this by the present model. Neither the octahedral charge nor the interlayer charge influence the optimum. The size of the octahedral cation, however, notably influences the octahedral rotation. If $r^{(6)}_{M-O}$ increases, a lower octahedral rotation is favored: with $b = 9.05$A and $r^{(6)}_{M-O} = 1.98$A about 6°, and with $b = 9.1$A and $r^{(6)}_{Fe-O} = 2.04$A about 4° octahedral rotation. This corresponds to the lower value in phengite when compared with muscovite, found in Güven's (1968) refinements.

If hydroxyl is replaced by fluorine, the minimum in O–O and F repulsion energy is less pronounced; the lower crystal energy is therefore obtained with octahedral rotations larger than 10°. A lesser ionic character of the Si–O bond slightly shifts this optimum to smaller octahedral rotation angles, because the tetrahedral contribution to the change in Coulomb energy is reduced. Due to a larger octahedral rotation, fluor-muscovite should have a larger basal spacing than a mica of otherwise equal composition; so far no literature has been found dealing with this subject.

More importantly, my calculations suggest that a larger octahedral cation reduces the optimum octahedral rotation. The size of the octahedral cation thereby will be found to influence the relative stability of the 1M and $2M_1$ polytypes.

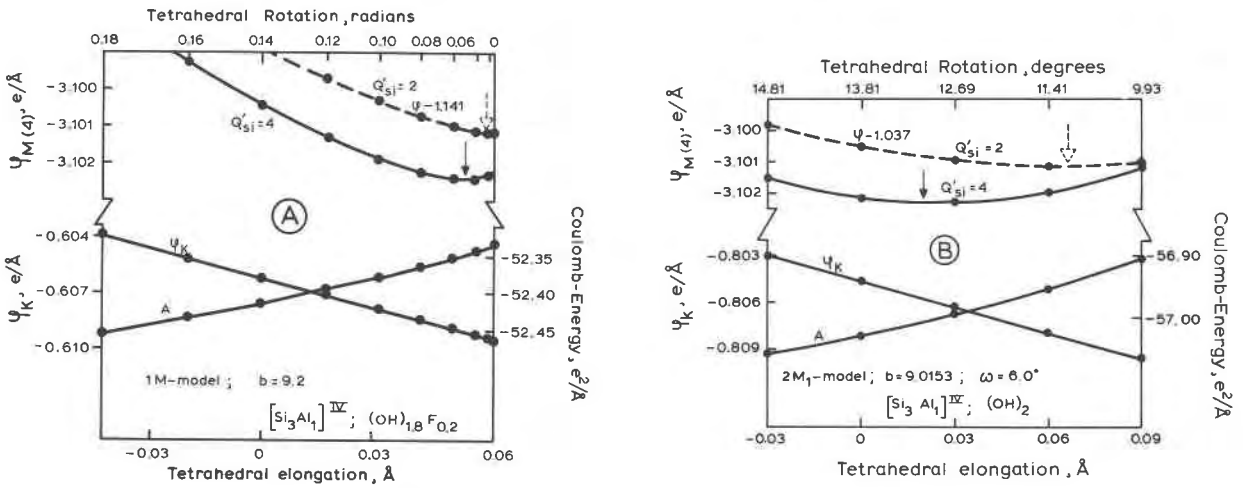

Fig. 2a and b. Coulomb energy of the 1M and $2M_1$ structures as a function of tetrahedral elongation/rotation. The optimum potential at the tetrahedral cation site shifts to larger elongations as the effective charge on this site decreases.

Tetrahedral rotation vs. elongation

It has been noted before that the tetrahedra in the mica structure tend to be elongated along c'. The elongation diminishes the basal edge-length, and thereby the tetrahedral rotation which is necessary for a structural fit of the octahedral and tetrahedral layer. With the coordination correction for the interlayer K–O bondlength (Appelo, 1978), the effect of elongation *vs.* rotation can be calculated for constant b and octahedral composition. Figure 2 shows that elongation decreases the Madelung sum, and the small increase in O–O and K–O repulsion energies make tetrahedral elongation even less favorable in terms of crystal energy.

The potential at the tetrahedral cation sites, however, shows well-defined minima with certain tetrahedral elongations. These minima are at an elongation of ~0.05 and 0.02A in the 1M and the $2M_1$ structural model, and shift to higher values with a higher imposed covalent character on the Si–O bond or with an increasing amount of Al(4). This suggested increase in tetrahedral elongation with increasing Al substituting for Si is reflected as a weak trend in structure refinements of similar micas, as shown for phlogopites in Figure 3.

It is interesting that the increasing tetrahedral rotation and a smaller K–O bondlength do not lower the potential at the interlayer ion site. The interlayer cation, therefore, has little importance in determining the tetrahedral rotation (*cf.* Radoslovich, 1962). The

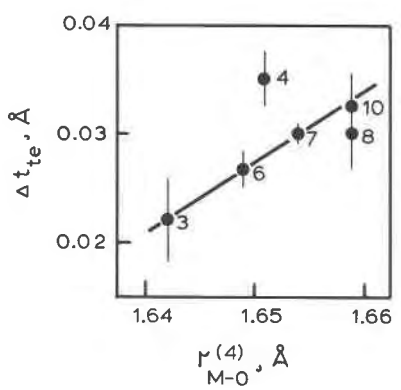

Fig. 3. In phlogopites, the tetrahedral elongation increases with larger tetrahedral cations, and implicitly lowers charge. The numbered micas are referenced under Fig. 5; 10 is biotite, with b = 9.23A, refined by Takeda and Ross (1975).

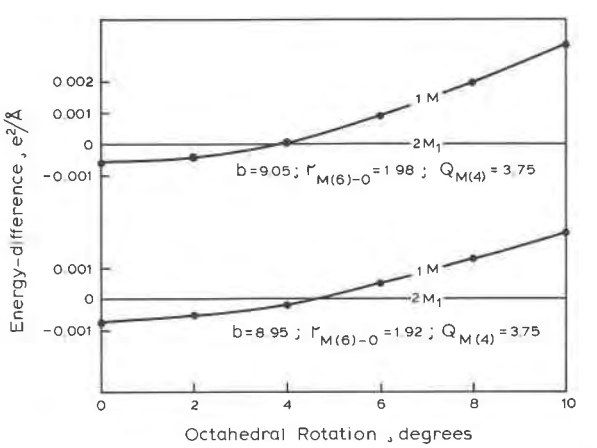

Fig. 4. The counter-rotation of upper and lower oxygen triads of the dioctahedral layer, and concomitant deformations in the tetrahedral layer determine the relative stability of 1M and $2M_1$ mica polytypes.

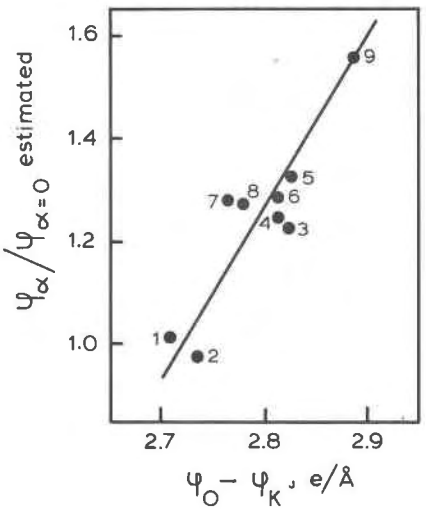

Fig. 5. A comparison of the potentials in the interlayer region ($\phi_O - \phi_K$) with relative values estimated with Pauling's coordination correction. The following refinements have been used: (1) Tepikin *et al.* (1969); (2) Hazen and Burnham (1973), annite; (3) McCauley *et al.* (1973); (4) Takeda and Donnay (1966); (5) Güven (1968), phengite; (6) Hazen and Burnham (1973), phlogopite; (7) Joswig (1972); (8) Rayner (1974); (9) Güven (1968), muscovite. Numbers increase with increasing tetrahedral rotation in the mica.

reason seems to be that the distance between the tetrahedral and interlayer cations shortens when the tetrahedral rotation increases at the expense of tetrahedral elongation.

Interlayer coordination: 1M and $2M_1$ polytypism

The mirror plane in the $2M_1$ model unit layer allows for a direct transformation into the 1M structure, and for the calculation of electrostatic energy differences which are the result of the stacking mode of the (dioctahedral) unit layers. Corrugation of the basal oxygens may act as a stabilizing factor in determining mica polytypism. In the dioctahedral mica, the corrugation can be ascribed geometrically to tetrahedral tilting which is a result of octahedral rotation, as this leads to unequal distances between the apical oxygens. The relative stability of the 1M and $2M_1$ polytypes is thereby related to the octahedral rotation, or counter-rotation of the upper and lower oxygen triads of the octahedra, which are shared with the tetrahedral layer. The electrostatic energy diffences of the two polytypes are shown in Figure 4 for fluor-mica.

The dioctahedral 1M structure is more stable up to an octahedral rotation of about 4° when compared with the dioctahedral $2M_1$ mica. The $2M_1$ structure is the more stable one for rotational values higher than 4°. The same results were obtained when the effective charge on Si was lowered to +2, and for micas when orientation and bondlength of O–H remained the same in both models.

The energy differences stem from the basal oxygens and tetrahedral cations (*not* from the interlayer cation), and they are small: less than 0.2 kcal/mole up to 6° octahedral rotation. All assumptions regarding bondlengths, ion positions, repulsive energy and ordering are the same for both structures. It therefore seems appropriate to transfer the energy differences directly into enthalpy and free-energy considerations of existing micas. Muscovite and phengite show octahedral rotations larger than 6° (Güven, 1968), and thus the $2M_1$ structure is favored. Synthesis of muscovite shows that crystal growth starts with the 1Md structure, which orders into 1M at lower temperatures and into $2M_1$ at higher temperatures (Yoder and Eugster, 1955; Velde, 1965). The same observations have been noted on illite in the natural environment (Dunoyer de Segonzac, 1969). 1M illite, however, is seldom found and may be limited to the diagenetic environment where Mg or Fe enters the octahedral layer in sufficient amounts to diminish the octahedral rotation. I consider here that it is mainly a larger $r^{(6)}_{M-O}$ that decreases the octahedral rotation and thereby favors the 1M polytype. The 1M structure of glauconite and celadonite (Burst, 1958; Hower, 1961; Wise and Eugster, 1964) is then seen to be related to the average $r^{(6)}_{M-O} = 2.03$Å, in contrast to illite, which has $r^{(6)}_{M-O} = 1.96$A [calculated from the average of the chemical formulas given by Weaver and Pollard (1973, Table 5, 16, 24), using *M*-O bond lengths quoted in part I].

Higher temperatures for a transition to the more stable polytype may be necessary to drive off interlayer water from expanded parts which are commonly associated with the 1Md structure (Maxwell and Hower, 1967). Such expanded parts, of course, reduce the energy differences between the stacking modes.

Electrostatic calculations of refined crystal data

The Madelung sums of seven 1M micas and two $2M_1$ micas refined by Güven (1968) have been calculated. The results can be used to investigate in more detail the proposed dependency of the interlayer K–O bondlength on the tetrahedral rotation (Appelo, 1978). Pauling's coordination correction can be rewritten to include the potential difference as:

Table 1. Comparison of structure and Coulomb energy of three representative 1M mica refinements and estimated structures

		x	y	z	Charge Q (e)	Potential ϕ (e/Å)	Estimated with b, c', α, z_O: Δ(Obs.-Est.).10^4 x	y	z	ϕ	Estimated with b, c', f_{Al}: Δ(Obs.-Est.).10^4 x	y	z	ϕ
PHLOGOPITE Joswig (1972)	K	0	0	0	0.92	-0.7778	-	-	-	18	-	-	-	-60
	H	0.098	0	0.3007	0.485	-0.8621	-23	-	3	-8	20	-	131	289
	M1(6)	0	0.5	0.5	2.025	-1.6574	-	-	-	13	-	-	-	-504
	M2(6)	0	0.1688	0.5	2.025	-1.6628	-	21	-	-41	-	21	-	-558
	M (4)	0.0755	0.3335	0.2257	3.7275	-3.0949	2	0.2	-1	9	10	0.2	27	301
	01	0.3255	0.26945	0.16768	-2.0	1.9863	1.8	0.1	(0.4)	17	27	21	13	2
	02	0.0171	0.5	0.1676	-2.0	1.9861	1	-	(-0.4)	11	-37	-	14	-8
	03	0.1307	0.33339	0.39097	-2.0	1.9243	4	0.6	(0)	27	13	0.6	35	-26
	04	0.1323	0	0.4009	-1.4375	1.3495	-13	-	(0)	-135	29	-	134	8
					Coulomb-energy	-50.4479 e^2/Å				-0.8				-719
F-PHLOGOPITE McCauley et al. (1973)	K	0	0	0	1.0	-0.8374	-	-	-	132	-	-	-	294
	M1(6)	0	0.5	0.5	2.0	-1.5641	-	-	-	-162	-	-	-	-558
	M2(6)	0	0.1694	0.5	2.0	-1.5608	-	27	-	-129	-	27	-	-524
	M (4)	0.0751	0.3337	0.2245	3.75	-3.1552	0	4	-7	184	1	4	3	65
	01	0.3208	0.2653	0.1682	-2.0	1.9841	-1	4	(2)	76	-24	-19	8	183
	02	0.0274	0.5	0.1678	-2.0	1.9945	11	-	(-2)	168	59	-	4	272
	03	0.1291	0.3339	0.3896	-2.0	1.9525	-8	6	(0)	-115	-9	6	8	-229
	F	0.1327	0	0.4017	-1.0	0.9048	-12	-	(0)	-240	27	-	129	1
					Coulomb-energy	-49.4084 e^2/Å				-155				-1330
ANNITE Hazen & Burnham (1973)	K	0	0	0	1.01	-0.7489	-	-	-	38	-	-	-	145
	H	(0.0891	0	0.2940)[a]	0.69	-1.1941	(0	-	0)	-20	-108	-	102	178
	M1(6)	0	0.5	0.5	2.1667	-1.7431	-	-	-	168	-	-	-	-542
	M2(6)	0	0.1668	0.5	2.1667	-1.7752	-	2	-	-153	-	-1	-	-859
	M (4)	0.0703	0.3335	0.2246	3.7025	-3.0773	-47	2	-4	21	-67	2	58	265
	01	0.3031	0.2543	0.1670	-2.0	1.9785	-67	4	(-7)	-28	-39	43	49	104
	02	0.0427	0.5	0.1684	-2.0	1.9966	-54	-	(7)	154	-143	-	63	285
	03	0.1291	0.3326	0.3894	-2.0	1.8954	-7	-7	(0)	-67	-56	-7	65	-86
	04	0.1239	0	0.3931	-1.85	1.6536	-71	-	(0)	-60	-108	-	102	21
					Coulomb-energy	-52.2724 e^2/Å				-66				-969

a) *Estimated*

$$\Sigma\phi_\alpha/\Sigma\phi_{\alpha=0} = (\sqrt{3} - \tan\alpha)/(\sqrt{3} + \tan\alpha)\{3.15/r_{K-O}^{(\alpha)}\}^7 \quad (1)$$

which includes the formal Born exponent 7. An expression for the "Madelung sum" or $\Sigma\phi$ of the interlayer region is the average potential of the three coordinating oxygens and of potassium: $\phi_O - \phi_K$. This is compared with the result of equation 1 in Figure 5. It shows an increase in $\phi_O - \phi_K$ with increasing tetrahedral rotation, which partly explains the low value of the Born exponent when $\phi_O - \phi_K$ is assumed constant. Although it is rather impractical to include $\phi_O - \phi_K$ in the coordination-correction equation, it increases R^2 to 0.988, as compared with $R^2 = 0.958$ without its inclusion in the same set of 9 micas. These data suggest a marked influence of simple Coulomb forces on bondlengths which is not yet fully explored.

Table 1 shows full results of the electrostatic calculations on three representative 1M micas. They are compared with model structures in which b, c', α and z_O are given (for lateral displacements) and with the model calculated from b, c' and $f_{Al}(4)$ as suggested in part I. In all structures the M2(6) ion is shifted along b; in combination with the shift of O4 (*i.e.* OH) along a, it gives this ion site a lower potential than the M1(6) site. Both sites are equal in the model structure, and a potential difference between the two sites may indicate ordering, even where such is not indicated by different bondlengths in the refinement. The M(4)–O3 bonds are relatively elongated in the actual structures, and thus are closer to the interlayer cation. This increases the potential at the interlayer site, when compared with the model structure. However, the displacements in the tetrahedral layer are generally within two e.s.d. of the refinement. An exception is the tetrahedron in annite (Hazen and Burnham, 1973), which is "sheared" along a. The reason is not clear; it nevertheless increases the Madelung sum, just as the other small displacements do in other "very close" refinements. The discrepancy in the Madelung sum becomes even larger when the structure is calculated from b, c', and the chemical analysis.

The same applies to Güven's $2M_1$ muscovite and phengite (Table 2). The discrepancies in these structures are, as noted before, the result of an overestimate of tetrahedral tilting and an underestimate of the octahedral rotation. The energy differences seem too high to warrant the use of these models in

Table 2. Comparison of structure and Coulomb energy of the two $2M_1$ micas refined by Güven (1968), with estimated structures

		x	y	z	Charge Q (e)	Potential ϕ (e/Å)		Δ(Obs.-Est.)·10⁴ x	y	z	ϕ
MUSCOVITE	K	0	0.0985	0.25	0.98	-0.8985		-	18	-	-61
	H	(0.3725	0.6504	0.0602)[a]	0.995	-1.5681		25	-36	-18	215
	M (6)	0.2496	0.0834	-0.00005	3.0	-2.3931		-4	-1	0	-440
	M1(4)	0.4648	0.9295	0.1355	3.755	-3.1181		-40	44	10	-42
	M2(4)	0.4510	0.2584	0.1355	3.755	-3.1189		-49	43	10	-49
	O1	0.4174	0.0930	0.1685	-2.0	1.9695		-16	41	18	-151
	O2	0.2513	0.8110	0.1575	-2.0	2.0236		5	4	-11	154
	O3	0.2522	0.3705	0.1689	-2.0	1.9700		-17	33	22	-185
	O4	0.4613	0.9435	0.0540	-2.0	2.0741		76	100	16	72
	O5	0.3850	0.2519	0.0537	-2.0	2.0723		-183	19	13	54
	O6	0.4564	0.5630	0.0505	-1.995	2.0611		-27	-36	-19	219
					Coulomb-energy	-56.9309 $e^2/Å$	b, c', β, f_{Al}				-1811
PHENGITE	K	0	0.0964	0.25	1.0	-0.8267		-	4	-	-243
	H	(0.3695	0.6528	0.0623)[a]	0.96	-1.5984		12	-25	8	368
	M (6)	0.2470	0.0825	0	2.85	-2.3404		-30	-8	0	123
	M1(4)	0.4632	0.9297	0.1355	3.88	-3.2262		-41	46	19	-294
	M2(4)	0.4525	0.2581	0.1354	3.81	-3.1571		-32	36	18	43
	O1	0.4426	0.0931	0.1678	-2.0	2.0603		23	37	23	-146
	O2	0.2372	0.8257	0.1601	-2.0	2.0744		-11	32	18	-82
	O3	0.2326	0.3574	0.1682	-2.0	2.0436		-85	11	27	-352
	O4	0.4568	0.9396	0.0544	-2.0	2.0201		51	78	23	152
	O5	0.3933	0.2496	0.0537	-2.0	2.0049		-129	-4	20	135
	O6	0.4531	0.5656	0.0526	-2.0	1.9717		14	-26	9	398
					Coulomb-energy	-57.5145 $e^2/Å$					-605

Estimated with

a) Estimated

the prediction of thermodynamic properties of individual minerals, if only a chemical analysis and unit-cell data are available.

Conclusions

When the absolute value of electrostatic calculations cannot be compared directly with sufficient experimental enthalpy values, it is to be weighted against other experimental data. It is then encouraging to find that the variation in the K–O bondlength in micas can be reproduced to within 99 percent of the experimentally-determined values by an electrostatic model. Such a high prediction ability points to other prediction possibilities, *e.g.* on element distributions among the rock-forming silicates. In the present study electrostatic calculations have been used in combination with structural models, which elucidated certain aspects of mica crystal-chemistry.

One of the more useful predictions is that a larger octahedral cation diminishes the distortion in the dioctahedral layer, and thereby favors the 1M polytype. This explains the exclusive occurrence of celadonite and glauconite as 1M polytypes, and affirms structural control (Smith and Yoder, 1956; Baronnet, 1974) to be a basic factor controlling mica polytypism.

Acknowledgments

I am indebted to Dr. R. M. Hazen for his positive criticism which resulted in a clarification of the text, and to Dr. H. A. van Lunsen who was so kind to polish the final English text. Thanks are also due to Professor Hartman for suggesting additional references.

References

Appelo, C. A. J. (1977) Layer-deformation and crystal-energy of trioctahedral 1M-micas and related minerals. *Proc. Int. Symp. Water-Rock Interaction, Strasbourg, IV,* 218–229.

——— (1978) Layer deformation and crystal energy of micas and related minerals. I. Structural models for 1M and $2M_1$ polytypes. *Am. Mineral., 63,* 782–792.

Baronnet, A. (1974) L'aspect croissance du polymorphisme et du polytypisme dans les micas synthétiques d'intérêt pétrologique. *Fortschr. Mineral., 52,* 203–216 (Special Issue, IMA Proceedings).

Bertaut, F. (1952) L'énergie électrostatique de réseaux ioniques. *J. phys. radium, 13,* 499–505.

Born, M. and K. Huang (1954) *Dynamical Theory of Crystal Lattices.* Oxford University Press, Oxford, England.

Born, L. and J. Zemann (1964) Abstandsberechnungen und gitterenergetische Rechnungen an Granaten. *Beitr. Mineral. Petrol., 10,* 2–23.

Burst, J. F. (1958) Mineral heterogeneity in 'glauconite' pellets. *Am. Mineral., 43,* 481–497.

Busing, W. R. (1970) An interpretation of the structures of alkaline earth chlorides in terms of interionic forces. *Trans. Am. Crystallogr. Assoc., 6,* 57–70.

Dunoyer de Segonzac, G. (1969) Les minéraux argileux dans la diagenèse—passage au métamorphisme. *Mém. Serv. géol. Als. Lorr., 29.* Strasbourg.

Ewald, P. P. (1921) Die Berechnung optischer und elektrostatischer Gitterpotentiale. *Ann. Physik, 64,* 253–287.

Felius, R. O. (1976) *Structural Morphology of Rutile and Trirutile Type Crystals.* Thesis, Leiden.

Gait, R. I. and F. B. Ferguson (1970) Electrostatic charge distributions in the structure of low albite. *Acta Crystallogr., B26,* 68.

Giese, R. F. (1971) Hydroxyl orientation in muscovite as indicated by electrostatic energy calculations. *Science, 172,* 263–264.

——— (1974) Surface energy calculations for muscovite. *Nature, 248,* 580–581.

——— (1975) The effect of F/OH substitution on some layer-silicate minerals. *Z. Kristallogr., 141,* 138–144.

Güven, N. (1968) The crystal structures of $2M_1$ phengite and $2M_1$ muscovite. *Carnegie Inst. Wash. Year Book, 66,* 487–492.

't Hart, J. (1978) *The Structural Morphology of Olivine-type Minerals.* Thesis, Leiden.

Hartman, P. (1972) *Structure and morphology.* In P. Hartman, Ed., *Crystal Growth: an Introduction,* p. 367–402. Elsevier, New York.

Hazen, R. M. and C. W. Burnham (1973) The crystal structures of one-layer phlogopite and annite. *Am. Mineral., 58,* 889–900.

Hougardy, J., D. Bonnin and A.-P. Legrand (1976) Estimation du potentiel électrostatique moyen de la vermiculite magnésienne de Llano par la méthode d'Ewald optimisée. *C. R. Acad. Sci. Paris, 283,* D1133–1136.

Hower, J. (1961) Some factors concerning the nature and origin of glauconite. *Am. Mineral., 46, 313–334.*

Joswig, W. (1972) Neutronenbeugungsmessungen an einem 1M-phlogopit. *Neues Jahrb. Mineral. Monatsh.,* 1–11.

Kittel, C. (1956) *Introduction to Solid State Physics, 2nd Ed.* Wiley, New York.

Maxwell, D. T. and H. Hower (1967) High-grade diagenesis and low-grade metamorphism of illite in the Precambrian Belt series. *Am. Mineral., 52,* 843–857.

McCauley, J. W., R. E. Newnham, and G. V. Gibbs (1973) Crystal structure analysis of synthetic fluorophlogopite. *Am. Mineral., 58,* 249–254.

Munoz, J. L. and S. D. Ludington (1974) Fluoride–hydroxyl exchange in biotite. *Am. J. Sci., 274,* 396–413.

Noda, T. and N. Yamanishi (1964) Hydrothermal synthesis of fluorine–hydroxyl–phlogopite. II Relationship between the fluorine content, lattice constants, and the conditions of synthesis of fluorine–hydroxyl–phlogopite. *Geochem. Int., 1964,* 96–104.

Ohashi, Y. and C. W. Burnham (1972) Electrostatic and repulsive energies of the M1 and M2 cation sites in pyroxenes. *J. Geophys. Res., 77,* 5761–5766.

Pauling, L. (1960) *The Nature of the Chemical Bond, 3rd Ed.* Cornell University Press.

Radoslovich, E. W. (1962) The cell dimensions and symmetry of layer-lattice silicates. II. Regression relations. *Am. Mineral., 47,* 617–636.

Rayner, J. H. (1974) The crystal structure of phlogopite by neutron diffraction. *Mineral. Mag., 39,* 850–856.

Sahl, K. and J. Zemann (1965) Gitterenergetische Rechnungen an Zirkon. Ein Beitrag zur Ladungsverteilung in der Silikatgruppe. *Tschermaks Mineral. Petrol. Mitt., 10,* 97–114.

Smith, J. V. and H. S. Yoder (1956) Experimental and theoretical studies of the mica polymorphs. *Mineral. Mag., 31,* 209–235.

Takeda, H. and J. D. H. Donnay (1966) Trioctahedral one-layer micas. III. Crystal structure of a synthetic lithium fluormica. *Acta Crystallogr., 20,* 638–646.

——— and M. Ross (1975) Mica polytypism: dissimilarities in the crystal structures of coexisting 1M and $2M_1$ biotite. *Am. Mineral., 60,* 1030–1040.

Tepikin, E. V., V. A. Drits and V. A. Alexandrova (1969) Crystal structure of iron biotite and construction of structural models for trioctahedral micas. *Proc. Int. Clay Conf., Tokyo, I,* 43–49.

Tosi, M. P. (1964) Cohesion of ionic solids in the Born model. *Solid State Phys., 16,* 1–120.

Tossell, J. A. (1977) A comparison of silicon–oxygen bonding in quartz and magnesian olivine from X-ray spectra and molecular orbital calculations. *Am. Mineral., 62,* 136–141.

Velde, B. (1965) Experimental determination of muscovite polymorph stabilities. *Am. Mineral., 50,* 436–449.

Verhoogen, J. (1958) Physical properties and bond type in Mg–Al oxides and silicates. *Am. Mineral., 43,* 552–579.

Waddington, T. C. (1959) Lattice energies and their significance in inorganic chemistry. *Adv. Inorg. Chem. Radiochem., 1,* 157–221.

Weaver, C. E. and L. D. Pollard (1973) *The Chemistry of Clay Minerals.* Elsevier, New York.

Wise, W. S. and H. P. Eugster (1964) Celadonite: synthesis, thermal stability and occurrences. *Am. Mineral., 49,* 1031–1083.

Yoder, H. S. and H. P. Eugster (1954) Phlogopite synthesis and stability range. *Geochim. Cosmochim. Acta, 6,* 157–185.

——— and ——— (1955) Synthetic and natural muscovites. *Geochim. Cosmochim. Acta, 8,* 225–280.

Manuscript received, March 13, 1978;
accepted for publication, July 11, 1978.